

Flexural behaviour of CFST members strengthened using CFRP composites

M.C. Sundarraja* and G. Ganesh Prabhu^a

¹ Thiagarajar College of Engineering, Madurai, Tamilnadu, INDIA

² Sethu Institute of Technology, Virudhunagar, Tamilnadu, INDIA

(Received May 09, 2011, Revised August 11, 2013, Accepted September 02, 2013)

Abstract. Concrete filled steel tubular members (CFST) become a popular choice for modern building construction due to their numerous structural benefits and at the same time aging of those structures and member deterioration are often reported. Therefore, actions like implement of new materials and strengthening techniques become essential to combat this problem. The application of carbon fibre reinforced polymer (CFRP) with concrete structures has been widely reported whereas researches related to strengthening of steel structures using fibre reinforced polymer (FRP) have been limited. The main objective of this study is to experimentally investigate the suitability of CFRP to strengthening of CFST members under flexure. There were three wrapping schemes such as Full wrapping at the bottom (fibre bonded throughout entire length of beam), U-wrapping (fibre bonded at the bottom throughout entire length and extended upto neutral axis) and Partial wrapping (fibre bonded in between loading points at the bottom) introduced. Beams strengthened by U-wrapping exhibited more enhancements in moment carrying capacity and stiffness compared to the beams strengthened by other wrapping schemes. The beams of partial wrapping exhibited delamination of fibre and were failed even before attaining the ultimate load of control beam. The test results showed that the presence of CFRP in the outer limits was significantly enhanced the moment carrying capacity and stiffness of the beam. Also, a non linear finite element model was developed using the software ANSYS 12.0 to validate the analytical results such as load-deformation and the corresponding failure modes.

Keywords: CFST members; CFRP fabrics; strengthening; flexure; externally bonded

1. Introduction

Composite construction may be considered as a reliable choice of attaining proper balance between the advantages it offers and the cost. An extensive variety of composite columns and beams are available nowadays, but the concrete filled steel tubular (CFST) sections are most commonly used (Zhao *et al.* 2010). Due to their excellent earthquake resistant structural properties such as high ductility, large energy absorption capacity and high-strength capacity, they are used in diversity of applications (De Nardin and El Debs 2007) but, at the same time, the ageing of above structures and its deterioration are often reported.

*Corresponding author, Ph.D., E-mail: mcsciv@tce.edu

Various strengthening or rehabilitation techniques such as section enlargement, external bonding of steel plates and fibers etc. has been proposed to overcome these problems. Among all strengthening methods, external strengthening provides a practical and cost effective solution.

The earliest generation utilized steel plates for external strengthening, but they had some harms such as heavy self weight, difficult in handling and susceptible to corrosion. Therefore, it is essential to implement new materials to combat this problem. The composite materials were introduced in the year of 1909 (Balazs and Borosnyol 2001, De Nardin and El Debs 2007), but, the composite industry began to bloom only after 1930s. Glass fibre reinforced polymers (GFRP) were first used in aircraft radar covers (Hollaway 1993) and at the end of 1930s, fibre reinforced polymer (FRP) boat hulls and car bodies were developed with glass fibres as the major reinforcement (Seica and Packer 2007). Since glass is a non-conductive material, it was used as an insulator to prevent galvanic corrosion of metals (Peters 1998). However, under certain conditions of exposure, glass fibres proved to be sensitive to alkaline environments and moisture attack (Reinhart 1998). At the end of 1960s, Royal Aircraft Establishment developed the carbon fibre reinforced polymer (CFRP) for special applications (Hollaway 1993). Unlike glass, carbon is an electrical conductor and hence galvanic corrosion could take place if carbon fibres are placed in direct contact with metals (Miller *et al.* 2001), but such fibres behave very well against creep deformation and relaxation (Balazs and Borosnyoi 2001). After the introduction of advanced composite materials in construction industry, the second generation utilized those materials for external strengthening of structures. External strengthening using FRP composites overcome the drawbacks exhibited by the steel plate bonding and also it offers numerous benefits such as flexibility to form any desired shape, high strength to weight ratio, cover more areas with limited access, excellent fatigue and creep resistance especially free from corrosion. The application of CFRP for the external strengthening of reinforced concrete (RC) structures has been widely carried out and reported in the past few decades (Teng *et al.* 2001). However, research related to FRP applications to steel structures has started quite recently and there are only few applications in practice due to uncertainties concerning the long term behaviour of these applications and the bonding between the composite materials and steel (Hollaway 1994, Zhao and Zhang 2007, Hollaway and Cadei 2002, Shaat *et al.* 2004).

One of the first known studies on this topic involved the use of CFRP laminates to repair steel structures conducted by Sen and Liby (1994). Six composite beams were tested under four-point loading. An epoxy adhesive was used to bond the CFRP laminates to the tension flange of the steel beam in different configurations. High strength steel bolts were also used in an attempt to transfer the load to CFRP laminates. The results indicated that even though significant ultimate strength was gained but more modest improvement in the elastic response are required. In another investigation, Jiao and Zhao (2004) studied 21 butt-welded very high strength (VHS) steel tubes strengthened with CFRP under axial tension. Three types of epoxy resins with different lap shear strength were used. Three kinds of failure modes such as adhesive failure, fiber tear and mixed failure were observed. The above investigation recommended a suitable epoxy adhesive and also concluded that a significant strength can be achieved by using CFRP–epoxy strengthening technique for strengthening of VHS steel tubes.

Photiou *et al.* (2006) investigated the effectiveness of an ultra-high modulus, and high modulus CFRP prepreg in strengthening the artificially degraded steel beam of rectangular cross-section under four-point loading by using two different wrapping configurations. The beam having ultra-high modulus CFRP was failed when the ultimate strain of the carbon fibre was reached in the pure moment region. The failure load exceeded the plastic collapse load of the undamaged

beam. The beams strengthened by using the high modulus CFRP exhibited ductile response leading to very high deflections even after higher ultimate load was reached and also neither fibre breakage nor adhesive failure was observed.

Seica and Packer (2007) investigated the FRP materials for the rehabilitation of steel tubular structures for underwater applications. Six tubes were wrapped with CFRP composites. In that two specimens were prepared under in-air conditions and remaining four were prepared under seawater curing conditions. Specimens were tested under four point loading. It was observed that the ultimate strength of the tubes wrapped under in-air and seawater curing conditions are 16-27% and 8-21% more than that of bare steel beam respectively. Tao and Han (2007) presented the results of axial compression and bending tests of fire-damaged concrete-filled steel tubes repaired using unidirectional CFRP composites. Both circular and square specimens were tested to investigate the repair effects of CFRP composites on them. The test results showed that the load-carrying capacity and the longitudinal stiffness of CFRP-repaired CFST stub columns increased while their ductility decreased with the increasing number of CFRP layers. In another study, Tao *et al.* (2008) repaired the fire-exposed CFST beams and columns by unidirectional CFRP composites. Both circular and square specimens were tested to investigate the repair effects of CFRP composites on them. The test results showed that the load-bearing capacity was enhanced by the fibre jackets to some extent, while the influence of CFRP repair on stiffness was not apparent.

From the past research, it can be observed that there have been investigations done with the use of CFRP as a strengthening material for metallic members and also presence of CFRP significantly enhance the behavior of steel tubular members. More research on CFRP strengthened steel tubular sections can be found in Shaat *et al.* (2004), Zhao *et al.* (2006), Haedir and Zhao (2010), Haedir *et al.* (2009). However research related to strengthening of CFST members using fibre is not widespread and also more tests are required to derive an optimal combination of fibre orientation, number of layers and sequence in applying CFRP layers. The main focus of the study is, to experimentally investigate the suitability of CFRP for strengthening of CFST members under flexural loading and also to compare the effectiveness of three possible geometric shapes of the fibre fabrics. Three types of wrapping schemes such as wrapping at the bottom (i.e., fibres were bonded at the bottom throughout full length of the steel tube), U-wrapping (i.e., fibres were bonded at the bottom throughout full length of the steel tube and extended the same up to the neutral axis) and partial wrapping (i.e., fibres were bonded in between loading points only at the bottom of steel tube) were used. Furthermore, to eliminate the galvanic corrosion between steel tube and CFRP, a thin layer of glass fibre mat was introduced between steel and CFRP. The new retrofitting technology could simplify the complicated and costly retrofitting methods used at present. By promoting the use of such a composite material in the retrofitting of steel structures, it leads to considerable short term and long term benefits.

Since the Finite Element Method (FEM) has reached a state of maturity, numerical simulation is an alternative method to validate with the experimental results and understand the behavior of CFRP strengthened CFST members. As a result, the present investigation also focused on modeling of CFRP strengthened beams using ANSYS 12.0. On the basis of experimental observations, a three-dimensional finite element model was developed to predict the load-deformation behavior of CFRP strengthened CFST members in which all the structural parameters and nonlinear properties of concrete, steel and FRP composites were considered.

2. Materials

2.1 Concrete

The concrete mix proportion designed by IS method to achieve the strength of 30 N/mm^2 and was 1:1.39:2.77 by weight. The designed water cement ratio was 0.35. Three cube specimens were cast and tested at the age of 28 days to determine the compressive strength of concrete. The average compressive strength of the concrete was 38.5 N/mm^2 .

2.2 Carbon fibre

The unidirectional carbon fibre called MBrace 240, fabricated by BASF India Inc was used in this study. It is a normal modulus CFRP fibre having modulus of elasticity of 240 kN/mm^2 and the tensile strength was 3800 N/mm^2 . The thickness and width of the fibre was 0.234mm and 600mm respectively. It is fabric type and can be tailored into any desired shape.

2.3 Adhesive

The MBrace saturant supplied by BASF India Inc was used in this study to get the good bonding between steel tube and carbon fibre. It is a two part systems, a resin and a hardener and the mixing ratio was 100:40 (B:H).

2.4 Steel tube

The square hollow steel tube confirming to IS 4923-1997 and IS 1161-1998 having a dimension of $91.5 \text{ mm} \times 91.5 \text{ mm}$ was used in this study. The thickness and length of the square hollow steel tube were 3.6 mm and 1500 mm respectively. The yield strength provided by the manufacturer was 250 N/mm^2 .

3. Experimental research

3.1 Specimen fabrication

The 1500 mm length square hollow tubes were cut from 6 m hollow tubes. To get the flat surface, both ends of the steel tube were surfaced by the surface grinding machine. Inside portion of the hollow steel tubes were thoroughly wire brushed to remove the rust and loose debris presented. Then the hollow steel tube specimens were filled with concrete and compacted by a steel rod to avoid any flaws or air gaps that occur inside the specimen. To eliminate the leakage of slurry during compaction, a steel plate was placed at the bottom prior to filling concrete. The concrete was cured for 28 days. Surface preparation of the metal substrate is very important to achieve good bonding between steel tube and CFRP fabrics. The strength of the adhesive bond is directly proportional to the quality of the surfaces to which it is bonded. So the exposed surface of the tubular specimen was blasted by the coarse sand to remove the rust and also to make the surface rough one. The CFST specimens after surface preparation are shown in Fig. 1. The entire sand blasted surface was cleaned by using acetone to remove all contaminant materials before retrofitted with the fibres. Prior to the beams strengthened by carbon fibre, the glass fibre fabric was introduced between the steel surface and CFRP composites to eliminate the galvanic corrosion. Finally, the carbon fibres were bonded to the exterior surface of the CFST members with the



Fig. 1 Concrete filled steel tubular specimens – after surface finishing



Fig. 2 Bonding of CFRP with the CFST specimen

different wrapping schemes and thicknesses. During wrapping of fibre fabrics, the resin and hardener are correctly proportioned and thoroughly mixed together and the excess epoxy and air were removed using a ribbed roller moving in the direction of the fibre. The bonding of FRP with the tubular sections is shown in Fig. 2.

3.2 Experimental setup

The two point loading system was adopted for the tests. A 16-Channel Data Acquisition System was used to store the data such as load and corresponding vertical deflection at three places. The beams were mounted over two pedestals kept at two ends of the beams and concentrated loads were applied by means of 50T hydraulic jack. Deflection measurements were taken by using linear voltage displacement transducers (LVDTs) and were kept at mid-span as well under the loading points. The load at which the CFRP starts rupturing, the failure load of the specimen and also the nature of failure were noted for each beam. The experimental setup is shown in the Fig. 3.

3.3 Description of specimens

Twenty seven beams, excluding three control beams were strengthened by FRP fabrics. Each



Fig. 3 Experimental setup

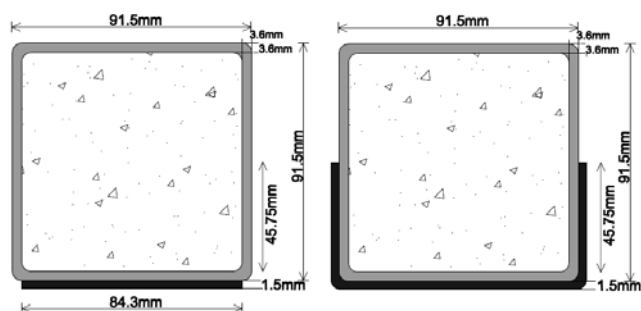


Fig. 4 Wrapping schemes

three beams were bonded externally by one, two and three layers of unidirectional CFRP fabrics in all wrapping schemes. The size and length of the beams were $91.5 \times 91.5 \times 3.6$ mm and 1500 mm respectively. To identify the specimen easily, the beams were designated with the names such as FUW-L1, FUW-L2, FUW-L3, FWB-L1, FWB-L2, FWB-L3, PWB-L1, PWB-L2 and PWB-L3. For example, the beams FUW-L2(3), FWB-L2(3) and PWB-L2(3) indicate that they were strengthened by using two layers of CFRP fabrics at the bottom only for entire length of beam, U-wrapping upto neutral axis throughout the entire length of beam and partial wrapping in between loading points at the bottom respectively and the numeral within the brackets indicates the number of specimen. The control (unbonded) beams were designated as CB1, CB2 and CB3. The wrapping schemes are shown in Fig. 4.

4. Results and discussion

4.1 Failure modes

Prior to apply loading, the specimens were placed at the supports and also centered to ensure symmetric loading. To understand the influence of CFRP on the flexural behavior of CFST members, the beams were loaded to until failure in quasi-static manner. The summary of test results such as failure modes and load at initial rupture were given in Table 1. The control specimens exhibited a smooth load-deflection curve with large deflection and ductility. The mid-span deflection of the beam exceeded 1/15 of the span at the end of the test. The failure mode of control specimen is shown in the Fig. 5. In all three wrapping schemes, the beams exhibited smooth load-deflection curve and followed half sine wave curve throughout the entire test which are shown in Figs. 6 to 8.

A small crushing sound was observed initially in the case of beams FWB-L1(1), FWB-L1(2) and FWB-L1(3) due to the removal of resin from them. All three beams exceeded their permissible limit of deflection after they reached load of 52 kN and then the beams are allowed to deflect. Finally, the failure occurred due to tearing of fibre at the centre of beams at the load of 120 kN as shown in Fig. A1 [Appendix A]. The beams strengthened with two layers of FRP such as FWB-L2(1), FWB-L2(2) and FWB-L2(3) exhibited the similar behavior observed in the beams strengthened with one layer but the failure load was higher. The failure pattern of beam with full wrapping of fibre at the bottom by two layers is shown in Fig. 9.



Fig. 5 Failure pattern of control beam

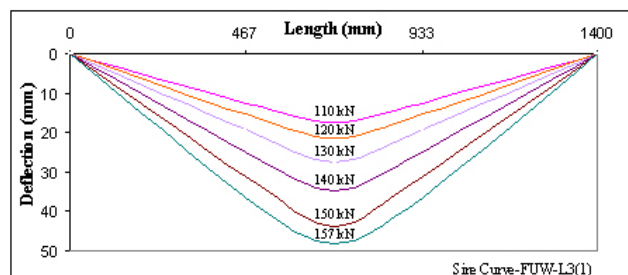


Fig. 6 Deflection along the beam FUW-L3(1) at different loading

Table 1 Failure load, moment carrying capacity and nature of failure of all specimens

1	2	3	4	5	6	7	8
CB-1	108.00	--	63.21	--	25.20	--	Large bending
CB-2	109.00	--	66.03	--	25.44	--	Large bending
CB-3	107.00	--	60.33	--	26.14	--	Large bending
FWB-L1(1)	113.00	101.00	37.39	90.26	26.37	3.67	Rupture of FRP between loading points and centre of specimen
FWB-L1(2)	115.00	102.00	35.32	115.07	26.84	5.50	Rupture of FRP at the centre
FWB-L1(3)	120.00	115.00	37.62	146.61	28.00	10.09	Rupture of FRP nearest to the loading point
FWB-L2(1)	119.00	101.00	33.94	148.68	27.77	9.17	Rupture of FRP between loading points and centre of specimen
FWB-L2(2)	122.00	92.00	37.19	159.78	28.47	11.93	Rupture of FRP started at the loading point and reached the centre of specimen
FWB-L2(3)	123.00	100.00	34.62	170.31	28.70	12.84	Rupture of FRP between loading points and centre of specimen
FWB-L3(1)	126.00	92.00	32.30	211.76	29.40	15.60	Rupture of FRP between loading points and centre of specimen and leads to debonding
FWB-L3(2)	148.00	114.00	43.62	261.07	34.54	35.78	Rupture of FRP at the loading points and moved towards the center as well the supports
FWB-L3(3)	140.00	115.00	42.31	199.65	32.67	28.44	Rupture of FRP between loading points and centre of specimen and leads to debonding
FUW-L1(1)	116.00	103	34.25	125.73	27.07	6.40	Tearing of fibres occurred at bottom and concentrated at centre of pure bending zone.
FUW-L1(2)	121.00	106	39.23	127.27	28.24	10.99	Tearing of fibres occurred at bottom and concentrated at centre of pure bending zone.
FUW-L1(3)	123.00	105	41.37	133.46	28.70	12.82	Tearing of fibres occurred at bottom and concentrated at centre of pure bending zone.
FUW-L2(1)	133.00	110	43.49	154.56	31.04	22.00	Tearing of fibres occurred at bottom and concentrated at loading point.
FUW-L2(2)	136.00	112	43.05	149.27	31.74	24.75	Tearing of fibres occurred at bottom and concentrated at centre of pure bending zone.
FUW-L2(3)	130.00	108	40.23	143.60	30.34	19.24	Tearing of fibres occurred at bottom and concentrated at loading point.
FUW-L3(1)	160.00	121	50.09	255.02	37.34	46.76	Tearing of fibres occurred at bottom and concentrated at centre of pure bending zone.

Table 1 Continued

FUW-L3(2)	154.00	118	48.6	272.67	35.94	41.26	Tearing of fibres occurred at bottom and concentrated at centre of pure bending zone.
FUW-L3(3)	148.00	116	42.12	248.83	34.54	35.75	Tearing of fibres occurred at bottom and concentrated at loading point.
PWB-L1(1)	103.00	101.00	26.42	59.57	24.04	-5.80	Abrupt complete delamination of fiber occurred before attaining ultimate load of control beam.
PWB-L1(2)	116.00	103.00	36.68	130.35	27.07	6.42	Abrupt complete delamination of fiber occurred before attaining ultimate load of control beam.
PWB-L1(3)	105.00	102.00	36.4	39.09	24.50	-3.80	Sudden complete delamination of fiber occurred before attaining ultimate load of control beam.
PWB-L2(1)	114.00	109.00	27.14	153.68	26.60	4.58	Abrupt complete delamination of fiber occurred and thrown off away from the beam
PWB-L2(2)	111.00	108.00	26.96	127.78	25.90	1.83	Abrupt complete delamination of fiber occurred and thrown off away from the beam
PWB-L2(3)	104.00	101.00	31.46	41.90	24.27	-4.80	Sudden complete delamination of fiber occurred before attaining ultimate load of control beam.
PWB-L3(1)	106.00	103.00	18.78	200.90	24.74	-2.83	Sudden complete delamination of fiber occurred before attaining ultimate load of control beam.
PWB-L3(2)	98.00	96.00	18.16	57.87	22.87	-11.22	Sudden complete delamination of fiber occurred before attaining load of control beam.
PWB-L3(3)	101.00	98.00	19.12	75.63	23.57	-7.92	Sudden complete delamination of fiber occurred before attaining ultimate load of control beam.

Among the beams strengthened with three layers of FRP by full wrapping at the bottom, the beams FWB-L3(2) and FWB-L3(3) exhibited the same behavior as observed in the beams strengthened with one layer and finally rupture of fibre was occurred with a huge sound when they attained the load of 148 kN and 140 kN respectively. But the beam FWB-L3(1) exhibited delamination of fibre throughout the entire length of the beam as shown in Fig. A2, in addition, the failure load was little higher than that of control beam. The delamination of fibre occurred due to failure of resin at the interface of steel tube and CFRP layer. From the above observations, it was concluded that there might be a possible bonding failure when the number of FRP layers increased.

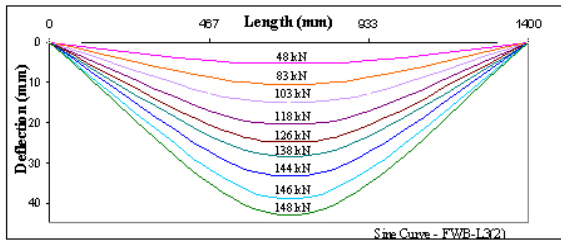


Fig. 7 Deflection along the beam FWB-L3(2) at different loading

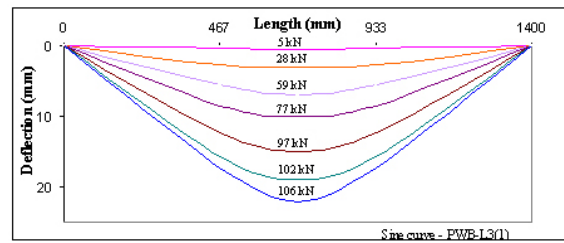


Fig. 8 Deflection along the beam PWB-L3(1) at different loading



Fig. 9 Failure pattern of beam FWB-L2(1)

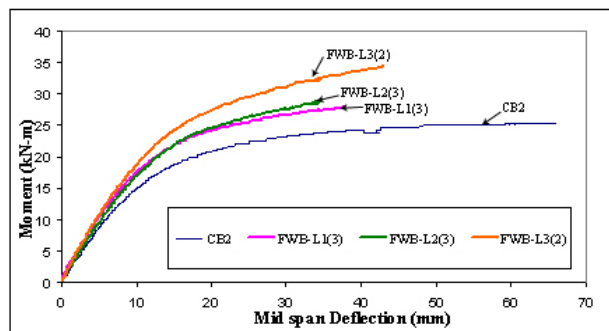


Fig. 10 Moment Vs Deflection of beams – FWB – comparison

Failure of beams FUV-L1(1), FUV-L1(2) and FUV-L1(3) occurred at the load of 116 kN, 121 kN and 123 kN respectively and at the same time, the deflection of the beams exceeded the limit of $1/30$. Until reach the failure load of control beam, no apparent debonding of fibre was identified. Therefore, a good composite action exist between the two components were confirmed. The rupture of fibre was occurred perpendicular to the orientation of the fibre at the bottom and extended on sides of beam when increasing the load further. The failure pattern of above beam is shown in Fig. A3. After rupture of CFRP, there is sudden drop in load observed due to the absence of tensile strength provided by the CFRP and finally the behaviour of beam observed was similar to that of control beam. The beams FUV-L2(1), FUV-L2(2) and FUV-L2(3) which were strengthened by U-wrapping scheme with two layers of fibre fabrics exhibited the similar behavior of beams strengthened by single layer but the failure load was high and the failure of beam is shown in Fig. A4. After they reached load of 110 kN, a non-linear response was observed and besides ductility enhancement was impaired.

The failure mode of beam with three layers of U-wrapping is shown in Fig. A5. The beams FUV-L3(1), FUV-L3(2) and FUV-L3(3) exhibited linear response behavior up to the load of 115 kN, and thereafter non-linear response was observed. The beam exceeded the permissible limit of deflection at the load of 65 kN. The mid span deflection was observed as 16.9 mm when they reached the failure load of control beam and also no failure of FRP was observed. The beam continued to deflect under the application of load further, tearing of fibres were occurred at a load of 160 kN, 154 kN and 148 kN for beams FUV-L3(1), FUV-L3(2) and FUV-L3(3) respectively and concentrated at centre of pure bending zone, furthermore, no tearing of fibres was observed on

either side of the beam.

At the initial stage, crushing sound of resin was observed in the case of beams with single layer of fibre bonded at the pure flexure zone [PWB-L1(1), PWB-L1(2) and PWB-L1(3)]. When loading further, the entire length of fibre got detached from the beam with huge sound and thrown off some distance away from the loading setup and it is shown in Fig. A6. After delamination of fibre was observed, the load got reduced and the strengthened beams behaved similar to control beam. The above same failure pattern was observed in the case of beams strengthened with two and three layers of FRP which are shown in Figs. A7 and A8 and at the same time, when increase in number of fibre layers, the delamination was occurred more rapidly and also the enhancement in the moment carrying capacity was very small. This delamination may attribute to discontinuity of the fibre and enormous amount of peeling stress was induced between fibre and steel at the edge. Crack patterns observed in all specimens are not unique and also no local buckling of steel tubes was observed at the compression zone of steel tube.

4.2 Moment deflection response

Table 1 summarizes the experimental test results such as the ultimate strength, maximum mid span deflection of all beams and also percentage increase in deflection control with respect to control beam (CB3). Moment-deflection behavior of CFRP strengthened beams with respect to control specimen is shown in Figs. 10 to 15. Until reach the failure load of control beam, all the strengthened beams under three wrapping schemes exhibited linear elastic behavior followed by inelastic behavior when increasing the load further. As expected, external bonding of CFRP significantly reduce the deflection and also enhance the stiffness of the beam compared to the control beam.

There is reduction in deflection observed in the case of beams strengthened by full wrapping at the bottom compared to control beam and is shown in Fig. 10. The percentage increase in deflection control of beams FWB-L1(3), FWB-L2(3) and FWB-L3(2) are 150%, 166% and 260% respectively compared to control beam (CB2) and their mid-span deflection at failure load of control beam observed are 24 mm, 22.5 mm and 16.7 mm respectively. It can be seen from the Fig. 16 that the enhancement in deflection control of specimen FWB-L3(2) is more than the specimens FWB-L1(3) and FWB-L2(3). And also, at the failure load of beams FWB-L1(3) and FWB-L2(3), the mid span deflection of the beam FWB-L3(2) observed was 37.62 mm and 34.62 mm respectively and the corresponding percentage of enhancement in deflection control was 78% and 51% respectively and is shown in Fig. 16.

The beam strengthened by U-wrapping significantly control the mid-span deflection compared to control beam as shown in Fig. 11. Comparing the behavior of beams FUW-L1(3), FUW-L2(2) and FUW-L3(1) to that of control beam (CB2), all three beams showed significant enhancement in stiffness and deflection control especially the behavior of FUW-L3(1) was outperformed. At failure load of control beam, the mid span deflection of beam FUW-L3(1) was 16.9mm and this deflection was 3.5 times lesser than that of control beam. The beams FUW-L1(3), FUW-L2(2) and FUW-L3(1) enhanced their deflection control by 134%, 150% and 256% respectively than control beam which is shown in Fig. 16. The above difference in deflection control attributed to the presence of number of CFRP layers in the outer limits and while increasing the number of layers, fibre lie in the outer limits provided required tensile capacity during large bending. Considering the increase in number of layers, the effect of single and two layers of FRP on deflection control was not obvious compared to the three layers and enhancement in deflection control was also not

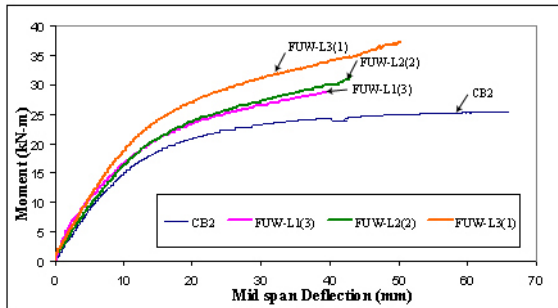


Fig. 11 Moment Vs Deflection of beams – FUW – comparison

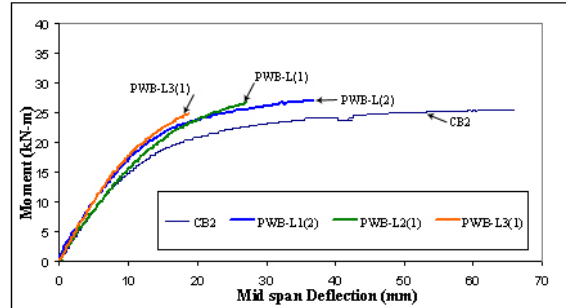


Fig. 12 Moment Vs Deflection of beams – PWB – comparison

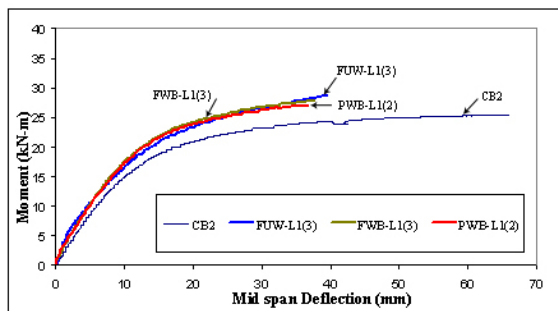


Fig. 13 Moment Vs Deflection of beams FWB-L1, FUW-L1 & PWB-L1 – comparison

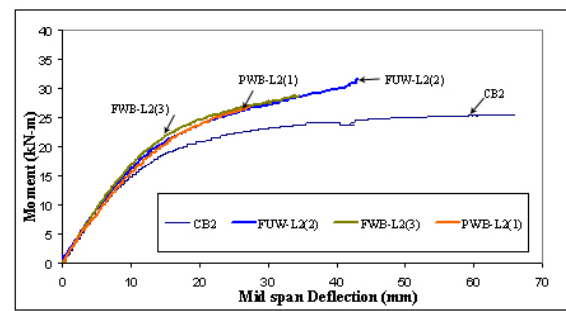


Fig. 14 Moment Vs Deflection of beams FWB-L2, FUW-L2 & PWB-L2 – comparison

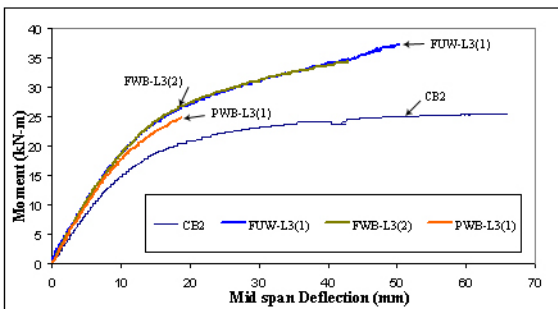


Fig. 15 Moment Vs deflection of beams FWB-L3, FUW-L3 & PWB-L3 – comparison

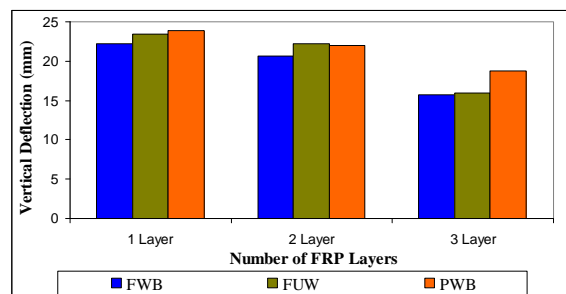


Fig. 16 Vertical deflection of all beams – comparison

proportional. From the Fig. 16, it can be seen that, beam FUW-L3(1), enhanced its deflection control by 70% and 37%, when compared to the beams FUW-L1(3) and FUW-L2(2) respectively.

Fig. 12 shows the moment deflection behavior of CFST beams strengthened by partial wrapping compared with the control specimen. In the case of beams strengthened with two and three layers of fibre, delamination was occurred before attaining the ultimate load of control beam. About 130.35%, 153.38% and 200.90% of reduction in deflection was observed in the case of

beams PWB-L1(2), PWB-L2(1) and PWB-L3(1) respectively when compared to that of control beam (CB2). Experimental results revealed that by increasing the number of FRP layers, the moment carrying capacity can be increased and at the same time, it proposed the delamination of fibre due to excessive development of peeling stress at the edge of the fibre. The enhancement in the control of deflection of beam PWB-L2(1) with respect to beam PWB-L1(2) was observed as 23.03%. From the Fig. 16, it can be seen that, with respect to the beam PWB-L1(2), 69.76% deflection was controlled in the case of beam strengthened with three layers of fibre (PWB-L3(1)).

Comparing the behavior of beams having U-wrapping with the beams having full wrapping at the bottom, beam strengthened by three layers in both wrapping exhibited identical load deflection behavior and also having significant effect on deflection control compared to the beams strengthened by one and two layers as shown in Figs. 13 to 15. Until reaching a load of 55 kN, the beams FUW-L1(3) and FUW-L2(2) followed the same path of FWB-L1(3) and FWB-L2(3) respectively, and thereafter a meager relaxation in deflection control was observed, and then exhibited more deflection control after attaining the load of 108 kN as shown in Figs. 13 and 14. This meager relaxation in deflection control in beam FUW-L1(3) and FUW-L2(2) attributed to the removal of resin at the interface between the steel tube substrate and the CFRP fabrics. The load deflection behavior of beam strengthened by partial wrapping followed the same path of beam strengthened by U-wrapping which is shown in Fig. 13. However, all beams in the case of partial wrapping exhibited delamination of fibre rather than rupture in addition some of the beams failed before attaining the ultimate load of control beam.

Comparing the behavior of beams strengthened by full wrapping and partial wrapping, the beams strengthened using full wrapping at the bottom exhibited more deflection control compared to the beams strengthened by partial wrapping. The moment-deflection response of beam PWB-L1(2) followed the same path of FWB-L1(3) and at the same time enhancement in deflection control of beam FWB-L1(3) was somewhat higher than that of PWB -L1(2) which is shown in Figs. 13 and 17. It was also observed that the difference in deflection control of beams PWB-L2(1) and PWB-L3(1) was very small when compared with the beams FWB-L2(3) and FWB-L3(3) respectively and at the same time it should be noted that the beam PWB-L3(1) was failed before attaining ultimate load of control beam (CB2). It can also be seen from the Fig. 17 that the deflection control of beams PWB-L1(3), PWB-L2(1) and PWB-L3(1) were decreased by 14.94%, 5.52% and 20.84% compared to the beams FWB-L1(3), FWB-L2(3) and FWB-L3(2)

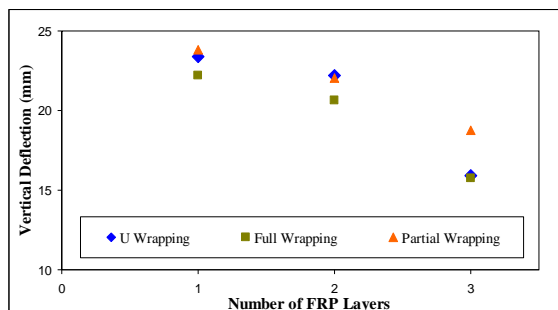


Fig. 17 Vertical deflection of beams – FUW, FWB & PWB - comparison

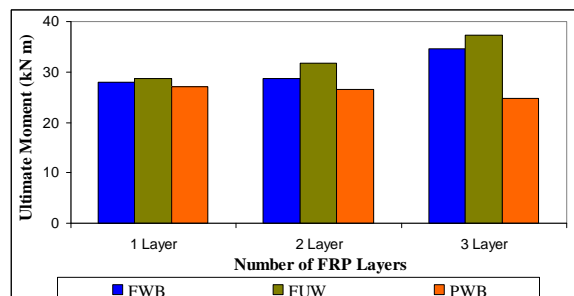


Fig. 18 Ultimate moment of all beams - comparison

respectively.

In overall, the beams FUW-L1(3), FUW-L2(2) and FUW-L3(1) enhanced 4%, 2% and 3% of deflection at the corresponding failure load of beams FWB-L1(3), FWB-L2(3) and FWB-L3(2) and also 15% 2% and 17% of deflection at the corresponding failure load of beam PWB-L1(3), PWB-L2(3) and PWB-L3(2) respectively as shown in Fig. 17. From the above observations, it is suggested that those beams subjected to large bending, the partial wrapping is not suitable for strengthening because of sudden delamination of fibre rather than rupture occurred and at the same time, if any appropriate anchorages like bolting or riveting will be provided to avoid debonding of fibre, then it will turn in to a fine and economical method for strengthening for CFST members.

4.3 Moment carrying capacity

The failure load, moment carrying capacity and percentage increase in moment carrying capacity of CFRP strengthened beams compared to the control beam are presented in Table 1. The main objective of this study is to enhance the flexural capacity of the CFST beams using CFRP fabrics. As expected the external bonding of fibre significantly increase the moment carrying capacity of the CFST beams especially for the beams strengthened by U-wrapping, nevertheless, the enhancement in moment carrying capacity of beams strengthened by partial wrapping was not considerable, especially for the beams strengthened by three layers.

Figs. 18 and 19 show the enhancement in moment carrying capacity of strengthened beams with respect to control beam. It can be seen from the Figs. 18 and 19 that the beams with full wrapping at the bottom showed the better enhancement in moment carrying capacity, especially, the beam bonded with three layers of CFRP [FWB-L3(2)] showed significant increase in moment carrying capacity compared to beams strengthened with one and two layers. Compared with control beam (CB2), the increase in moment carrying capacity of beams FWB-L1(3), FWB-L2(3) and FWB-L3(2) were found to be 10.1%, 12.84%, 35.77% respectively. In all beams, the increase in moment carrying capacity was not linear with respect to increase in number of layers and furthermore, this observation is fairly agreed with the beam strengthened by U-wrapping.

The results obtained from U-wrapping technique revealed that, presence of CFRP in the outer limits considerably increase the moment carrying capacity of the beam especially for the beam strengthened by three layers as shown in Fig. 18. The increase in moment carrying capacity of beams FUW-L1(3), FUW-L2(2) and FUW-L3(1) were found to be 13%, 25%, and 47% more than that of control beam (CB2). It can be seen from Figs. 18 and 19 that, improvement in moment carrying capacity was not linear when increasing the number of layers. Only 10.5% increase in moment carrying capacity was observed while increasing the CFRP layer from one to two whereas 17.6% increase in moment carrying capacity was observed while increasing the number of layers from two to three. This low enhancement in moment carrying capacity for two layers may be due to presence of thin fibre layer in the outer limits which is not able to generate required tensile capacity during bending.

The failure mode of all specimens strengthened by partial wrapping scheme was observed as delamination of fibre and in few beams, it was occurred before reaching the ultimate load of control beam. Enhancement in moment carrying of beams with partial wrapping compared to the control beam is shown in Figs. 18 and 19. From that Figs. 18 and 19, it was observed that the moment carrying capacity of the beam with three layers of fibres got reduced due to sudden detachment of fibre from the specimen. Comparing the behaviour of PWB-L1(2) and PWB-L2(1) to that of control beam CB2, only 6.4% and 4.58% respectively of moment carrying capacity was

enhanced.

Out of three wrapping schemes, the beams strengthened using U-wrapping scheme showed better improvement in moment carrying capacity compared to the beam strengthened by flat wrapping at the bottom and it is shown in Fig. 19. However the deflection control of the beams FUW-L1(3) and FUW-L2(2) was less than that of FWB-L1(3) and FWB-L2(3) respectively but the moment carrying capacity increased by 3% and 10.5% respectively. It can be seen from the Fig. 19 that the beam FUW-L3(1) exhibited 8.1% increase in moment carrying capacity compared to beam FWB-L3(2) even though their load deflection behavior are same. This enhancement in moment carrying capacity under U- wrapping scheme is due to the presence of fibres at the web of the CFST member to resist the applied load initially and delayed the load transfer to the fibre at the bottom as a result the rupture of fibre was postponed. Compared with the beams strengthened by partial wrapping scheme, enhancement in moment carrying capacity of beams strengthened by U-wrapping were outperformed which is shown in Fig. 19. The moment carrying capacity of beam PWB-L1(2) is nearly equal to that of beam FWB-L1(3) but the moment carrying capacity of beam PWB-L2(1) and PWB-L3(1) were decreased by 7.89% and 39.64% compared to the beam FWB-L2(3) and FWB-L3(2) respectively. This is due to the sudden removal of fibre and completely detached and thrown off away from the specimen.

From the above observations, it is recommended that those beam subjected to large bending, the U-wrapping and Full wrapping scheme is suitable for strengthening and furthermore a better care should be taken like bolting or riveting to eliminate the delamination of fibre in the case of beams with partial wrapping and to enhance the moment carrying capacity further.

4.4 Ductility response

Ductility is defined as the material can be able to plastically deform without any breaking. Ductility index of the control and CFRP strengthened beams had been found as per Zhong Tao and shown in Figs. 20 to 22. It has been found that the control specimen exhibited more ductile nature compared to CFRP strengthened beams and also the ductility of the strengthened specimens decreased when the number of FRP layers increased. This decrease in ductility is due to the sudden rupture of CFRP fabrics. It can be seen from the Fig. 22 that, the beams strengthened by FRP fabrics at the bottom showed better ductility response than that of beams with U-wrapping scheme.

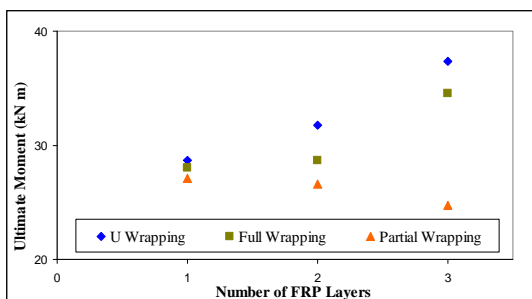


Fig. 19 Ultimate moment of all beams - FUW, FWB & PWB - comparison

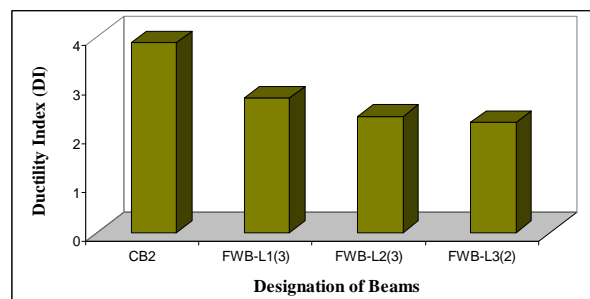


Fig. 20 Ductility index of beams – FWB – comparison

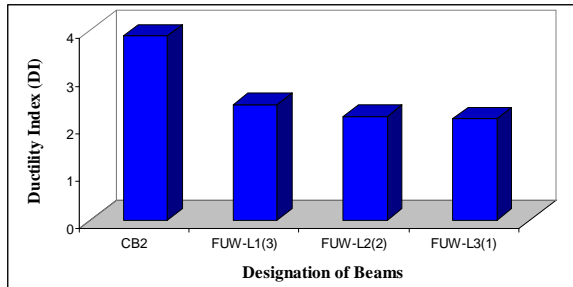


Fig. 21 Ductility index of beams – FUB – comparison

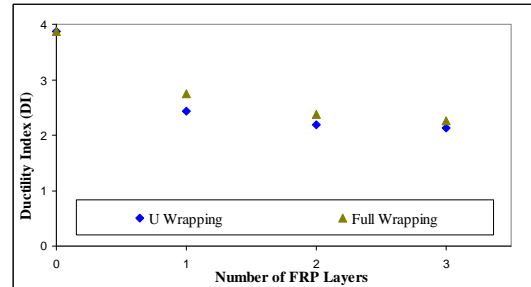


Fig. 22 Ductility index of beams – FWB & FUB – comparison

5. Finite element modeling

5.1 Element types and end constraints

The finite element package ANSYS 12.0 offers a variety of options such as element types, numerical solution controls, auto-meshers, and sophisticated postprocessors and graphics to speed the analyses. In this paper, three dimensional nonlinear finite element models were created by using finite element package ANSYS 12.0 to validate the experimental results of the CFRP strengthened concrete filled steel tubular members. The dimension of the of the steel tube and CFRP thickness were used in the numerical modeling based on the measured cross sectional dimension of the specimen.

An eight-node solid element (Solid65) was used to model the concrete core of the CFT member. The element is defined by eight nodes having three degrees of freedom at each node i.e translations in the nodal directions x, y, and z. The element is similar to the Solid45 (3-D Structural Solid) element with the addition of special cracking and crushing capabilities. The element is capable of creep, plastic deformation, cracking in three orthogonal directions, and crushing. An eight-node solid element (Solid45) was used for modeling the steel tubes and CFRP composites. The element is defined with eight nodes having three degrees of freedom at each node and eight translations in the nodal directions x, y, and z.

Regarding the application of load, concentrated loads are applied incrementally by means of an equivalent displacement to overcome convergence problems. Point loads are applied at 1/3 span of the steel tube from both the ends. Whenever the solution dose not converges for the set of parameters considered, as far as load step size and convergence criterion is concerned. In order to model the simply supported beam condition, the vertical displacement (Y) of the bottom flange of steel tube or fibre nodes was restrained and also all rotational degrees of freedom were released to allow for rotation. Fig. 23 shows the loading and boundary condition assigned to the beam.

5.2 Material properties

The concrete behavior is modeled by a multi-linear isotropic hardening relationship and the compressive strength of the concrete is taken as the actual cube strength of the concrete. The Poisson's ratio of the concrete was assumed as 0.2 and the modulus of elasticity was evaluated by

the following as per IS 456:2000.

$$E = 5000\sqrt{f_{ck}} \quad (1)$$

f_{ck} = 28 days cube compressive strength of concrete.

The uniaxial stress-strain relationship of the concrete was constructed by compression. Fig. 24 shows the uniaxial stress-strain relationship of concrete and that was used in this study.

$$f = \frac{E_c \varepsilon}{1 + \left(\frac{\varepsilon}{\varepsilon_o}\right)^2} \quad (2)$$

$$\varepsilon_o = \frac{2f'_c}{E_c} \quad (3)$$

$$E_c = \frac{f}{\varepsilon} \quad (4)$$

where

- E_c = Elastic modulus of concrete
- f'_c = Ultimate uniaxial compressive strength
- f = Stress at any strain ε
- ε = Strain at stress of f
- ε_o = Strain at the ultimate compressive strength

The isotropic properties such as Young's modulus and Poisson's ratio of the mild steel tubes were approximately considered as 210 GPa, and 0.3 respectively. The non-linear behavior of steel was considered in this study by specifying yield stress and tangent modulus. The tangent modulus of the steel was assumed as 0.3 percentage of its young's modulus and the yield stress was 320 MPa.

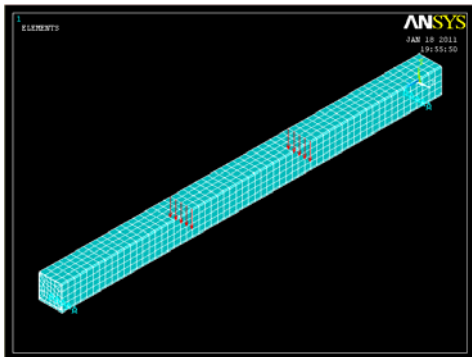


Fig. 23 Typical loading and boundary condition assigned to beam in ANSYS 12.0

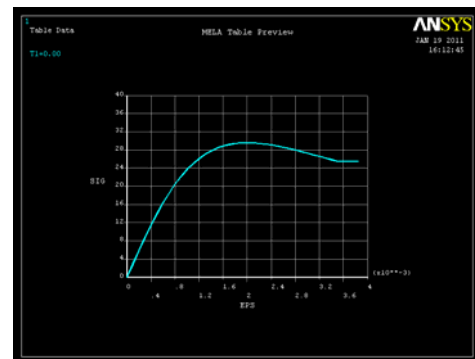


Fig. 24 Stress-strain relationship assigned to the concrete model in ANSYS 12.0

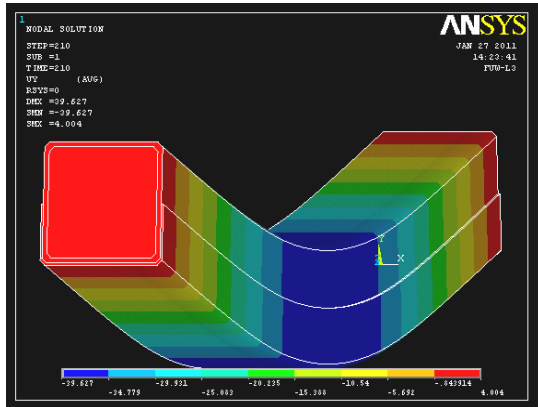


Fig. 25 Failure pattern of FUW-L3 by numerical simulation (ANSYS 12.0)

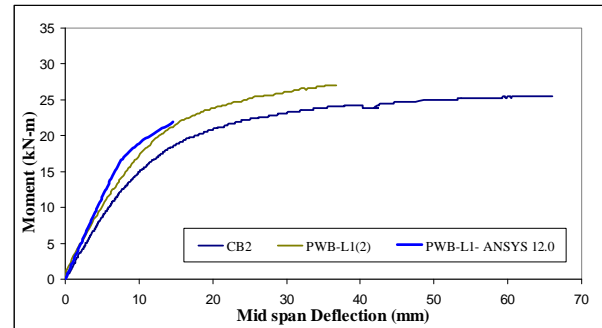


Fig. 26 Comparison of experimental and computed load–deformation curves for PWB-L1(2)

The FRP composites are considered as an orthotropic material, that is, their properties are not same in all directions. The thickness of single composite layer was 0.5 mm and the unidirectional elastic properties namely Young's modulus and Poisson's ratio were assigned as 240 GPa and 0.22 respectively. For analysis, the density of concrete, steel and CFRP was 2500 kg/m^3 , 7850 kg/m^3 and 1720 kg/m^3 respectively.

5.3 Numerical results

The nonlinear solution of the simulated models was run in ANSYS 12.0 and results obtained from numerical study are fairly matching the results of experimental study. The deformed shapes of the beams obtained by numerical simulation were fairly agreed with the corresponding experimental results. In addition, the deflected shapes of the beams followed the half sine wave curve throughout the entire test as shown in Fig. 25 which is similar to that of experimental investigation.

The time-displacement behaviour of CFRP strengthened beams which were simulated by ANSYS 12.0. Moment-deflection behavior of CFRP strengthened beams were also compared with the experimental results and are represented in Fig. 26 and also in Figs. B1 to B8 [Appendix B]. As expected, external bonding of CFRP significantly reduced the deflection and enhanced the stiffness of the beam which was observed both in modeling and also in experimentation. The load deflection curve obtained by numerical simulation for all strengthened beams exhibited linear elastic behavior until reach the failure load of control beam followed by inelastic behavior when increasing the load further. In addition to that, behavior of those had good agreement with the experimental results. In all strengthened beams, the deflection obtained in the case of computational graphs is 2 mm to 3 mm less than that of experimental results until reach the yield point.

Failure load obtained from numerical simulation was found to be 10% to 15% more than that of experimental results in both the wrapping schemes except in the case of beam strengthened by single layer which was 10% less than that of the experimental values.

6. Conclusions

There were three wrapping schemes such as full wrapping at the bottom throughout the entire length of the beam, U-wrapping upto the neutral axis and partial wrapping at pure bending zone introduced. These wrapping schemes are proposed for further improvement of moment carrying capacity and also to control the deflection of the CFST beams. From the experimental data obtained, the failure modes, moment-deflection behaviour, ultimate moment carrying capacity and effect of ductility response were discussed. Finally, a non linear finite element model was developed using the software ANSYS 12.0 to validate the analytical results such as load-deformation and the corresponding failure modes. Based on the flexural tests on twenty seven specimens wrapped with CFRP fabrics, the following conclusions can be made:

- Until reach the failure load of control beam, all the strengthened beams under three wrapping schemes exhibited linear elastic behavior followed by inelastic behavior when increasing the load further. As expected, external bonding of CFRP significantly reduce the deflection and also enhance the stiffness of the beam compared to the control beam.
- A good composite action exist between two components were confirmed in the case of beams with full wrapping at the bottom and U-wrapping schemes and no apparent debonding of fibre was identified whereas the beams of partial wrapping exhibited delamination of fibre and were failed even before attaining the ultimate load of control beam and at the same time, if any appropriate anchorages like bolting or riveting are provided to avoid debonding of fibre, then it will turn in to a fine and economical method for strengthening for CFST members.
- The percentage increase in deflection control of beams FWB-L1(3), FWB-L2(3) and FWB-L3(2) are 150%, 166% and 260% respectively whereas in the case of beams FUW-L1(3), FUW-L2(2) and FUW-L3(1) it was 134%,150% and 256% respectively compared to control beam (CB2).
- Out of three wrapping schemes, the beams strengthened using U-wrapping scheme showed better improvement in moment carrying capacity compared to the beams strengthened by flat wrapping at the bottom; however the deflection control of the beams FUW-L1(3) and FUW-L2(2) was less than that of FWB-L1(3) and FWB-L2(3) respectively.
- The control specimens exhibited more ductile nature compared to CFRP strengthened beams and also the ductility of the strengthened specimens decreased when the number of FRP layers increased. The beams strengthened by FRP fabrics at the bottom showed better ductility response than that of beams with U-wrapping scheme.
- The load deflection curve obtained by numerical simulation for all strengthened beams exhibited linear elastic behavior until reach the failure load of control beam followed by inelastic behavior when increasing the load further. In addition to that, behavior of those had good agreement with the experimental results.
- As expected, external bonding of CFRP significantly reduced the deflection and also enhanced the moment carrying capacity and stiffness of the beam which was observed both in modeling and also in experimentation.

Acknowledgments

This research work has been carried out through the research fund [File No.35-112/2008 (SR)] received from University Grants Commission, New Delhi, India under Major Research Project

scheme.

References

- Balazs, G.L. and Borosnyoi, A. (2001), "Long-term behavior of FRP", *Proceedings of the International Workshop on Composites in Construction: A Reality*, American Society of Civil Engineers, VA, 84-91.
- De Nardin, S. and El Debs, A.L.H.C. (2007), "Axial load behaviour of concrete-filled Steel tubular columns", *Proceedings of the Institution of Civil Engineers – Structures & Buildings*, February, **160**(1), SB1 13-22.
- Haedir, J. and Zhao, X.L. (2010), "Design of short CFRP-reinforced steel tubular columns", *J. Constr. Steel Res.*, **67**(3), 497-509.
- Haedir, J., Bambach, M.R., Zhao, X.L. and Grzebieta, R.H. (2009), "Strength of circular hollow sections (CHS) tubular beams externally reinforced by carbon FRP sheets in pure bending", *Thin-Wall. Struct.*, **47**(10), 1136-1147.
- Hollaway, L. (1993), *Polymer Composites for Civil and Structural Engineering*, Blackie Academic and Professional, Glasgow, UK.
- Hollaway, L. (1994), *Handbook of Polymer Composites for Engineers*, Woodhead Publishing Ltd., Cambridge, UK.
- Hollaway, L.C. and Cadei, J. (2002), "Progress in the technique of upgrading metallic structures with advanced polymer composites", *Progress in Struct. Eng. Mater.*, **4**(2), 131-148.
- Jiao, H. and Zhao, X.L. (2004), "CFRP strengthened butt-welded very high strength (VHS) circular steel tubes", *Thin-Wall. Struct.*, **42**(7), 963-978.
- Miller, T.C., Chajes, M.J., Mertz, D.R. and Hastings, J.N. (2001), "Strengthening of a steel bridge girder using CFRP plates", *ASCE J Bridge Eng.*, **6**(6), 514-522.
- Photiou, N.K., Hollaway, L.C. and Chryssanthopoulos, M.K. (2006), "Strengthening of an Artificially Degraded Steel Beam Utilizing a Carbon/Glass Composite System", *Constr. Build. Mater.*, **20**(1-2), 11-21.
- Peters, S. (1998), *Handbook of Composites*, Chapman & Hall, London, UK.
- Reinhart, T.J. (1998), *Overview of Composite Materials*, Chapman & Hall, London, UK.
- Seica, M.V. and Packer, J.A. (2007), "FRP materials for the rehabilitation of tubular steel structures, for underwater applications", *Compos. Struct.*, **80**(3), 440-450.
- Sen, R. and Liby, L. (1994), "Repair of steel composite bridge sections using CFRP laminates", *U.S. Department of Transportation Contract B- 7932*, University of South Florida, Tampa, FL, USA.
- Shaat, A. and Fam, A. (2006), "Axial loading tests on CFRP-retrofitted short and long HSS steel columns", *Can. J. Civil Eng.*, **33**(4), 458-470.
- Shaat A., Schnersch, D., Fam, A. and Rizkalla, S. (2004), "Retrofit of steel structures using fiber-reinforced polymers (FRP): State-of-the-art", *Transportation Research Board (TRB) Annual Meeting*, Washington, January.
- Tao, Z. and Han, L.H. (2007), "Behaviour of fire-exposed concrete-filled steel tubular beam columns repaired with CFRP wraps", *Thin-Wall. Struct.*, **45**(1), 63-76.
- Tao, Z., Han, L.H. and Zhuang, J.P. (2008), "Cyclic performance of fire-damaged concrete-filled steel tubular beam-columns repaired with CFRP wraps", *J. Constr. Steel Res.*, **64**(1), 37-50.
- Teng, J.G., Chen, J.F., Smith, S.T. and Lam, L. (2001), *FRP-Strengthened RC Structures*, John Wiley & Sons, West Sussex.
- Zhao, X.L. and Zhang, L. (2007), "State of the art review on FRP strengthened steel structures", *Eng. Struct.*, **29**(8), 1808-1823.
- Zhao, X.L., Fernando, D. and Al-Mahaidi, R. (2006), "CFRP strengthened RHS subjected to transverse end bearing force", *Eng. Struct.*, **28**(11), 1555-1565.

Appendix A

Fig. A1 Failure Pattern of beam FWB-L1(2)



Fig. A2 Failure Pattern of beam FWB-L3(1)



Fig. A3 Failure Pattern of beam FUW-L1(3)



Fig. A4 Failure Pattern of beam FUW-L2(1)



Fig. A5 Failure Pattern of beam FUW-L3(1)



Fig. A6 Failure Pattern of beam PWB-L1(1)



Fig. A7 Failure Pattern of beam PWB-L2(3)



Fig. A8 Failure Pattern of beam PWB-L3(3)

Appendix B

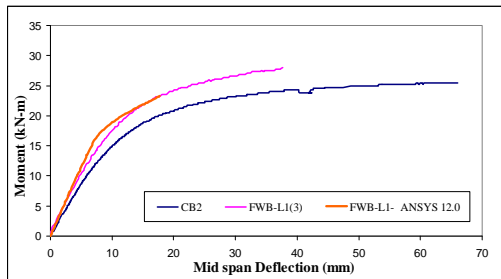


Fig. B1 Comparison of experimental and computed load–deformation curves for FWB-L1

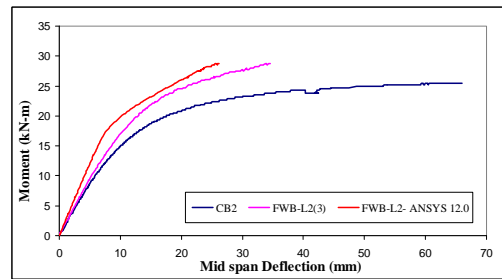


Fig. B2 Comparison of experimental and computed load–deformation curves for FWB-L2

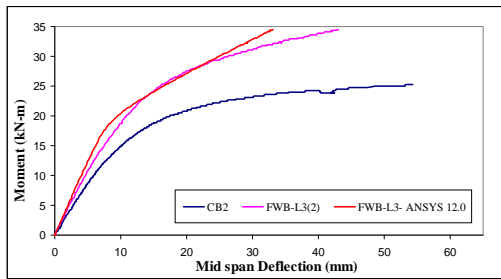


Fig. B3 Comparison of experimental and computed load–deformation curves for FWB-L3

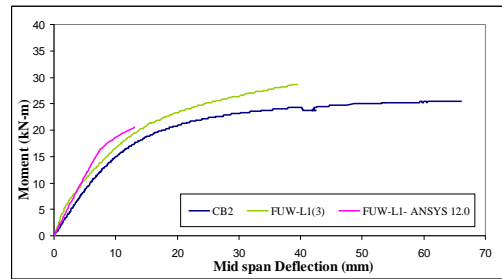


Fig. B4 Comparison of experimental and computed load–deformation curves for FUW-L1

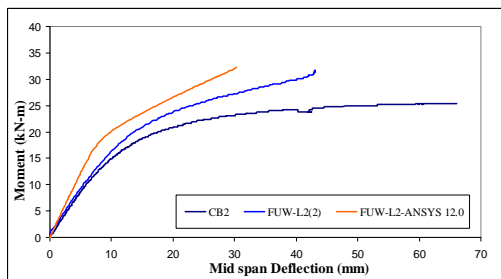


Fig. B5 Comparison of experimental and computed load–deformation curves for FUW-L2

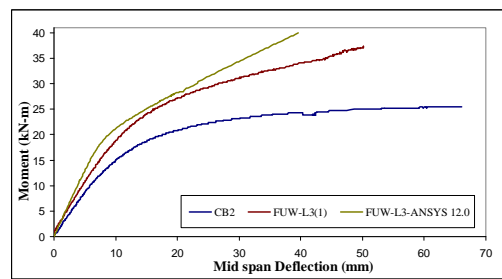


Fig. B6 Comparison of experimental and computed load–deformation curves for FUW-L3

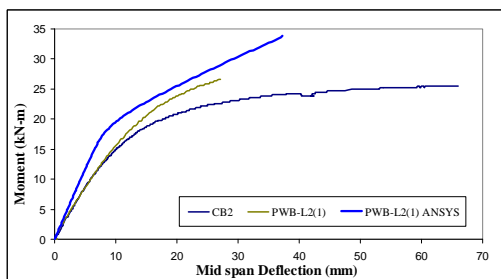


Fig. B7 Comparison of experimental and computed load–deformation curves for PWB-L2(1)

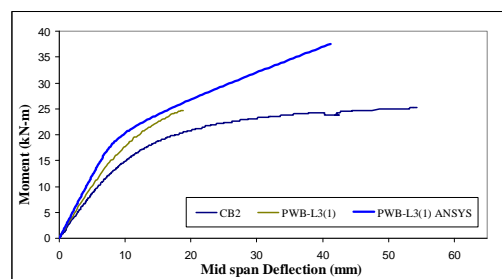


Fig. B8 Comparison of experimental and computed load–deformation curves for PWB-L3(1)